APPLICATION OF TRIAXIAL COMPRESSION TEST RESULTS TO THE CALCULATION OF FLEXIBLE PAVEMENT THICKNESS

By E. S. Barber

Highway Engineer, Public Roads Administration

SYNOPSIS

While service records and field observations are recognized as essential to the design of bases and surfaces, theoretical relations between pavement performance and soil characteristics are presented as an aid to interpreting and evaluating field data.

The stresses and displacements resulting from a uniform vertical pressure over a circular area are tabulated. Also discussed are the variations caused by time-consolidation, contact shear stress, elliptical contact area, rigidity of bearing area, and strength of supporting material.

Stress-strain and strength characteristics of pavement and foundation materials are determined from triaxial test results and applied to the calculation of pavement thickness by three methods: (1) Displacement, which requires empirical determination of allowable displacement; (2) overstress of a point, applicable to cohesive materials; (3) bearing capacity, applicable to both cohesive and cohesionless materials.

The variation of pavement thickness with load and moisture content of a cohesive subgrade is illustrated. It is suggested that the effect of the pavement on the strength of the subgrade may be as important as its affect on the stress distribution.

Stresses transmitted from a uniform tangential stress over a circular area such as caused by vehicle deceleration are evaluated. A relation between such loading and surface thickness is presented.

The selection of thickness of flexible pavement (surface and base) required to support a given loading over a given subgrade is generally based on service records and observations of field performance of similar pavements constructed on similar subgrades. To evaluate the similarity of various pavement materials and subgrades, a method of testing the materials is necessary. In correlating observations of pavement performance involving various loads and materials, it is helpful to have a theoretical relationship between the pavement thickness and the material test results.

Thus, while the results of field observations are required, their application may be broadened and their evaluation made more quantitative if they are correlated by means of test results on the component materials with the aid of theoretical relationships. The following discussion concerns several relationships between triaxial compression test results and pavement thickness based on stress distribution in elastic materials and the strength of plastic materials.

ELASTIC STRESS DISTRIBUTION

Figure 1 shows the stresses acting on an element in a semi-infinite elastic mass subjected at the surface to a uniform pressure over a circular area. The shear stress acting vertically in the tangential plane is equal to the horizontal radial shear stress. The horizontal tangential normal stress is a principal stress; there are no shear stresses in the plane on which it acts.

These stresses have been evaluated analytically by Love (*1*)[1] and tabulated numerically by Tufts (*2*). Some corrections were made to Tufts' tabulation by means of influence charts (*3*) to derive Table 1, which shows the ratio of these stresses to the applied pressure for various depths and radial distances

[1] Italicized numbers in parentheses refer to list of references at the end of the paper.

measured from the center of the loaded area in terms of its radius. The vertical normal stress and the horizontal radial shear stress are independent of Poisson's ratio (ratio of lateral to axial strain in a simple compression test). The radial and tangential normal stresses are given for Poisson's ratio of 0 and 0.5. Stresses for Poisson's ratio other than 0 and 0.5 may be obtained by direct interpolation, thus the stress for a Poisson's ratio 0.25 is halfway between the tabulated values.

Integration of the stresses shown in Table 1 gives the vertical displacement factors

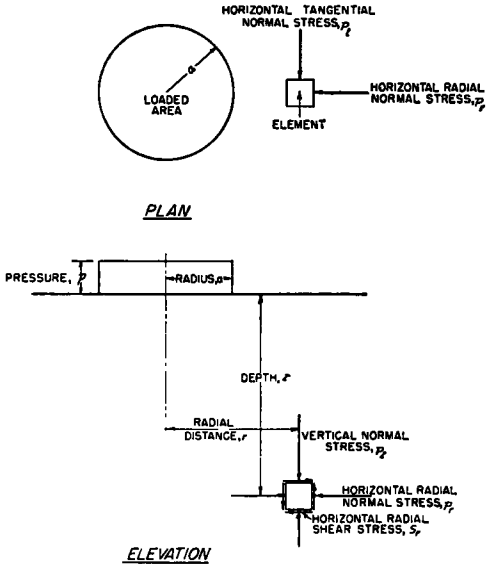

Figure 1. Stresses from Applied Pressure

shown in Table 2. While the stresses in a homogeneous mass are independent of the modulus of elasticity, the displacement is inversely proportional to the modulus. The displacement may be divided into two parts—that due to volume change only, corresponding to Poisson's ratio = 0; and that due to lateral displacement at constant volume corresponding to Poisson's ratio = 0.5.

In comparing displacements in field tests with calculated values, consideration must be given to the fact that displacement due to volume change of wet soils is delayed because of the time required for the stress to be transferred to the soil solids as part of the water is forced out. This time effect and its dependence upon the permeability of the surface (*4*) is illustrated in Figure 2. The curves on the left represent settlements when the surface is pervious, those on the right show the settlements at the same time when no drainage can occur at the surface. The relation between stress, volume change, and time for soil samples is determined in the consolidation test whereby a disk of soil is encircled with a metal ring and compressed between two pervious plates.

The time effect must also be considered when viscous materials are loaded. Under constant pressure, the surface displacement outside the loaded area may increase at first and then decrease as the displacement under the load continues to increase (*5*).

Figure 3, Case I, shows the deflection of the surface of an elastic mass caused by a uniform pressure. If the supporting material is overstressed by a uniform pressure, the edge deflection increases and may exceed that at the center as indicated in Figure 3, Case II, for cohesionless support. If an elastic circular bearing block is placed between a uniform pressure and an elastic support, the reaction is concentrated toward the edge of the block (*6*). As the rigidity of the block increases, the edge stress increases without limit giving a uniform displacement (Case III, Figure 3) equal to 0.923 times the average displacement under a uniform pressure or 0.785 times the axial displacement under a uniform pressure (Case I, Figure 3). Because of the lack of bearing capacity of unconfined cohesionless material, a rigid block on the surface of sand produces a reaction concentrated on the axis of loading (Case IV, Figure 3).

The reaction under smooth-faced rollers and wheels without pneumatic tires approaches that shown in Case V, Figure 3, under a rigid solid cylinder. The average reaction is 0.785 times the maximum reaction (*7*).

The maximum reaction is

$$\sqrt{\frac{P'E}{R(1-\mu^2)}}$$

where:

P' = load per unit length
R = radius of loading cylinder
E = modulus of elasticity of the elastic support
μ = Poisson's ratio of the elastic support

TABLE 1

RATIO OF STRESSES TRANSMITTED TO A POINT IN A SEMI-INFINITE MASS FROM A SURFACE LOAD UNIFORMLY DISTRIBUTED OVER A CIRCULAR AREA

Depth of point ÷ radius	Horizontal radial distance ÷ radius, $\frac{r}{a}$								
	0	0.25	0.5	1.0	1.5	2.0	2.5	3.0	4.0
Vertical normal stress transmitted to point ÷ pressure applied at surface, $\frac{p_z}{p}$									
$\frac{z}{a}$									
0.25	0.986	0.983	0.964	0.460	0.015	0.002	.000	.000	.000
0.5	.911	.895	.840	.418	.060	.010	.003	.000	.000
0.75	.784	.762	.691	.374	.105	.025	.010	.002	.000
1.0	.646	.625	.560	.335	.125	.043	.016	.007	.000
1.25	.524	.508	.455	.295	.135	.057	.023	.010	.001
1.5	.444	.413	.374	.256	.137	.064	.029	.013	.002
1.75	.346	.336	.309	.223	.135	.071	.037	.018	.004
2.0	.284	.277	.258	.194	.127	.073	.041	.022	.006
2.5	.200	.196	.186	.150	.109	.073	.044	.028	.011
3	.146	.143	.137	.117	.091	.066	.045	.031	.015
4	.087	.086	.083	.076	.061	.052	.041	.031	.018
5	.057	.057	.056	.052	.045	.039	.033	.027	.018
Horizontal radial normal stress ÷ applied pressure (Poisson's ratio = 0.5) $\frac{p_r}{p}$									
0.25	0.643	0.626	0.565	0.385	0.144	0.058	0.028	0.014	0.004
0.5	.374	.360	.325	.286	.196	.098	.050	.027	.008
0.75	.208	.204	.196	.209	.175	.112	.064	.044	.012
1.0	.116	.118	.123	.149	.146	.104	.069	.045	.022
1.25	.067	.072	.080	.107	.116	.096	.069	.047	.026
1.5	.040	.046	.055	.078	.091	.082	.064	.047	.026
1.75	.025	.028	.035	.056	.070	.068	.058	.046	.027
2.0	.016	.019	.024	.041	.053	.057	.052	.042	.027
2.5	.008	.009	.013	.023	.033	.038	.038	.035	.025
3	.004	.006	.008	.014	.021	.026	.028	.026	.022
4	.001	.002	.003	.006	.009	.012	.015	.016	.016
5	.001	.001	.002	.003	.005	.007	.008	.009	.010
Horizontal tangential normal stress ÷ applied pressure (Poisson's ratio = 0.5) $\frac{p_t}{p}$									
0.25	0.643	0.628	0.580	0.243	0.019	0.005	0.001	0.000	0.000
0.5	.374	.359	.317	.141	.028	.007	.003	.001	.000
0.75	.208	.197	.170	.085	.025	.008	.003	.001	.000
1.0	.116	.109	.096	.054	.021	.008	.003	.001	.000
1.25	.067	.063	.056	.035	.016	.007	.003	.001	.000
1.5	.040	.037	.034	.023	.012	.006	.003	.001	.000
1.75	.025	.024	.022	.015	.009	.005	.003	.001	.000
2.0	.016	.015	.014	.011	.007	.004	.002	.001	.000
2.5	.008	.007	.007	.006	.004	.003	.002	.001	.000
3	.004	.004	.003	.003	.002	.002	.001	.001	.000
4	.001	.001	.001	.001	.001	.001	.000	.000	.000
5	.001	.001	.000	.000	.000	.000	.000	.000	.000
Horizontal radial shear stress at point ÷ pressure applied at surface, $\frac{s_r}{p}$									
0.25	0.000	0.024	0.065	0.299	0.042	0.014	0.003	0.002	0.001
0.50	.000	.057	.129	.262	.102	.032	.013	.006	.002
0.75	.000	.069	.141	.221	.128	.053	.024	.013	.003
1.00	.000	.065	.124	.178	.128	.069	.033	.018	.007
1.25	.000	.053	.101	.146	.118	.072	.039	.023	.010
1.50	.000	.041	.080	.119	.104	.071	.045	.028	.012
1.75	.000	.033	.062	.094	.091	.068	.046	.030	.014
2.00	.000	.026	.048	.070	.078	.062	.045	.032	.015
2.5	.000	.016	.030	.050	.056	.050	.041	.032	.018
3	.000	.009	.019	.034	.040	.040	.035	.029	.018
4	.000	.005	.009	.018	.022	.024	.024	.022	.016
5	.000	.002	.005	.010	.013	.015	.016	.016	.013

TABLE 1—*Concluded*

Depth of point ÷ radius	Horizontal radial distance ÷ radius, $\frac{r}{a}$								
	0	0.25	0.5	1.0	1.5	2.0	2.5	3.0	4.0
	Horizontal radial normal stress ÷ applied pressure (Poisson's ratio = 0) $\frac{p_r}{p}$								
0.25	0.265	0.248	0.199	0.082	−0.026	−0.045	−0.061	−0.046	−0.026
0.50	.098	.087	.063	.075	.056	−.006	−.016	−.018	−.017
0.75	.008	.008	.009	.055	.067	.033	.009	.000	−.010
1.00	−.030[a]	−.025	−.015	.033	.058	.041	.021	.008	.000
1.25	−.043	−.036	−.024	.018	.044	.040	.026	.015	.004
1.50	−.044	−.038	−.028	.007	.032	.035	.027	.019	.006
1.75	−.041	−.036	−.028	−.001	.022	.028	.025	.019	.009
2.00	−.037	−.033	−.024	−.006	.013	.022	.022	.019	.010
2.5	−.028	−.026	−.022	−.010	.004	.012	.016	.016	.011
3	−.022	−.020	−.017	−.010	−.002	.006	.010	.011	.010
4	−.014	−.012	−.011	−.009	−.004	−.001	.003	.005	.007
5	−.009	−.009	−.008	−.007	−.004	−.002	.000	.001	.004
	Horizontal tangential normal stress ÷ applied pressure (Poisson's ratio = 0) $\frac{p_t}{p}$								
0.25	0.265	0.259	0.245	0.183	0.132	0.095	0.061	0.046	0.026
0.50	.098	.094	.085	.070	.074	.061	.048	.037	.022
0.75	.008	.007	.007	.017	.034	.038	.034	.029	.019
1.00	−.030	−.030	−.025	−.009	.011	.020	.023	.021	.016
1.25	−.043	−.042	−.037	−.021	−.002	.009	.014	.015	.013
1.50	−.044	−.043	−.039	−.025	−.010	.001	.007	.010	.010
1.75	−.041	−.040	−.037	−.026	−.013	−.003	.003	.006	.008
2.00	−.037	−.036	−.033	−.025	−.015	−.007	−.001	.003	.006
2.5	−.028	−.028	−.026	−.022	−.015	−.010	−.004	−.001	.002
3	−.022	−.021	−.020	−.018	−.014	−.010	−.006	−.004	.000
4	−.014	−.014	−.014	−.012	−.010	−.008	−.006	−.005	−.002
5	−.009	−.009	−.009	−.009	−.008	−.007	−.006	−.005	−.002

[a] Minus sign indicates tensile stress.

TABLE 2

DISPLACEMENT FACTORS DUE TO UNIFORM PRESSURE OVER CIRCULAR AREA

$$\text{Displacement } S = \frac{\text{pressure} \times \text{radius}}{\text{modulus of elasticity}} \text{ factor} = \frac{pa}{E} F$$

Depth of point ÷ radius	Horizontal radial distance ÷ radius, $\frac{r}{a}$										
	0	.25	.50	.75	1.00	1.25	1.5	2	2.5	3	4
	Displacement factor for Poisson's ratio = 0.5, $\frac{SE}{pa}$										
$\frac{z}{a}$											
0	1.50	1.48	1.40	1.25	0.95	0.66	0.54	0.39	0.30	0.26	0.18
0.5	1.34	1.31	1.23	1.09	0.89	0.68	0.55	0.40	0.31	0.27	0.19
1	1.06	1.05	0.98	0.89	0.78	0.66	0.56	0.41	0.32	0.27	0.19
1.5	0.83	0.83	0.79	0.73	0.67	0.60	0.52	0.40	0.32	0.28	0.20
2	0.67	0.67	0.65	0.62	0.57	0.53	0.48	0.39	0.32	0.28	0.20
3	0.47	0.47	0.46	0.45	0.43	0.41	0.38	0.34	0.30	0.27	0.21
4	0.36	0.36	0.35	0.35	0.34	0.33	0.32	0.30	0.28	0.25	0.20
5	0.29	0.29	0.29	0.29	0.29	0.28	0.28	0.25	0.24	0.23	0.19
	Displacement factor for Poisson's ratio = 0, $\frac{SE}{pa}$										
0	2.00	1.97	1.86	1.67	1.27	0.88	0.71	0.52	0.41	0 34	0.25
0.5	1.51	1.49	1 39	1.24	1.06	0.85	0.68	0.51	0.41	0.34	0.25
1	1.12	1.11	1 04	0 94	0.85	0.74	0.65	0.50	0.40	0.34	0.25
1.5	0.86	0.85	0.81	0.76	0.70	0.65	0 59	0 47	0.39	0.34	0.25
2	0.68	0.67	0.65	0.62	0.59	0.55	0.52	0.44	0.38	0.33	0.25
3	0.48	0.47	0.46	0.45	0.44	0.42	0.40	0.37	0.33	0.30	0.24
4	0.37	0.36	0.35	0.35	0.35	0.34	0.33	0.31	0.29	0.26	0.22
5	0.29	0.29	0.29	0.29	0.29	0.28	0.28	0.26	0.25	0.24	0.20

The reaction thus increases with increases in the load and modulus of elasticity, E, and decreases with increases in the radius, R.

Another factor which must be considered in evaluating loading tests is the production of inward acting shear stresses at the surface under pneumatic tires (*8*). While measured shear stresses show a maximum at the quarter

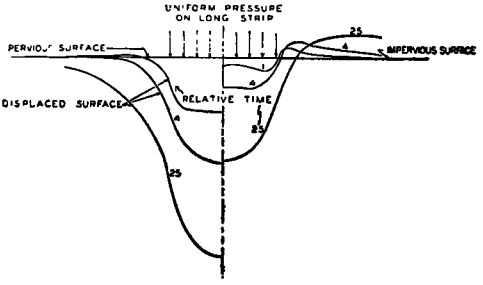

Figure 2. Effect of Time of Consolidation on Displacement of a Loaded Surface

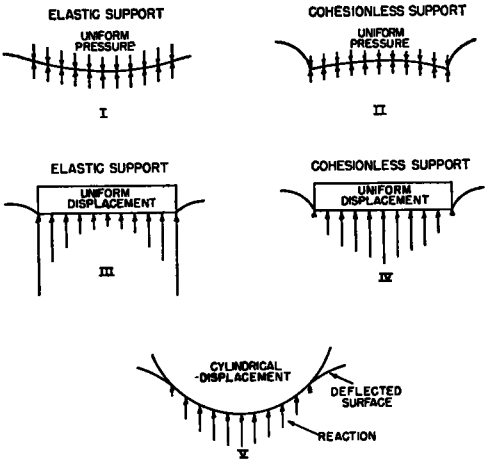

Figure 3. Reactions Under Surface Loads

points of the diameter of the loaded area their effect may be approximated by the vertical normal stress and displacement shown in Figure 4 for a uniformly applied shear stress (*9*). These normal stresses added to those due to the vertical applied pressures could account for the fact that Spangler measured pressures transmitted to a strong base through a surface course which were greater than the inflation pressure of the tire used for applying the load (*10*). The shear stress also tends to increase the axial displacement more than that at the edge.

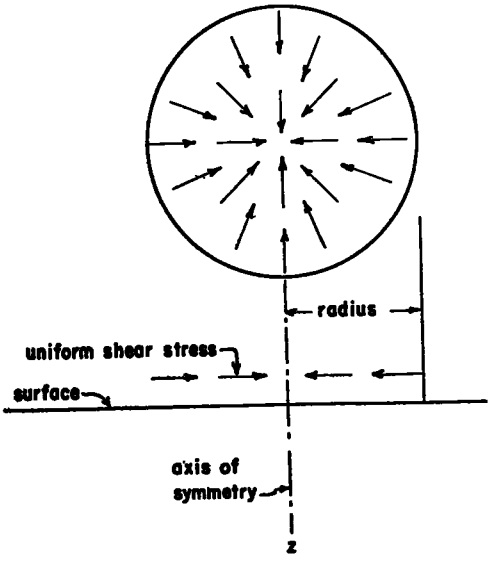

Depth of point ÷ radius	Vertical normal stress ÷ applied stress	Displacement factor[a] (Poisson's ratio = 0)
0	1.00	1.00
0.25	0.91	0.76
0.5	0.72	0.55
1	0.35	0.29
1.5	0.17	0.17
2	0.09	0.11
3	0.03	0.05
5	0.01	0.02

[a] Displacement = $\frac{\text{shear stress} \times \text{radius}}{\text{modulus of elasticity}}$ factor

Figure 4. Axial Vertical Stress and Displacement Under Uniform Shear Stress Applied Over Circular Area

The theoretical surface displacements for three distributions of vertically applied pressure (*11*) are shown in Figure 5. A uniform pressure over an elliptical area slightly smaller (about 10 percent) than the contact area is a good approximation of measured vertical pressures under pneumatic tires (*12*). While the displacement is different on the major and minor axes, the average displacement is very close to that for a uniform pressure over a circular area.

In the following discussion, the load, P,

is considered as the inflation pressure of the loaded tire, p, applied vertically and uniformly distributed over a circular area of radius, a, giving the relation $P = p\pi a^2$.

STRESSES AT A POINT

The stresses shown in Figure 1 and Table 1 are those acting at a point in the vertical and horizontal directions. The stresses at a point in other directions can be calculated from those given in Table 1. Thus, for a point with coordinates $\frac{z}{a} = 3$ and $\frac{r}{a} = 2$ with Poisson's ratio = 0.5, Table 1 gives $\frac{p_z}{p} = 0.066$, $\frac{p_r}{p} = 0.026$, and $\frac{s_r}{p} = 0.040$. The average normal stress is the average of the normal stresses in any two mutually perpendicular directions, which for this point is $\frac{0.066 + 0.026}{2} = 0.046$.

The average normal stress is plotted in Figure 6 as point O on the horizontal or normal stress axis. A point representing the normal and shear stress on one plane is plotted as A in Figure 6 for the plane perpendicular to the radial direction with an abscissa of 0.026 and an ordinate of 0.040. With O as a center and OA as radius, a semicircle is drawn. Any point B on this semicircle (Mohr's circle of stress) represents the stresses acting on a plane making an angle of $\frac{1}{2}$ AOB with the plane of the stresses represented by point A. The intersections of the semicircle with the normal stress axis determine the principal stresses at the point. These principal stresses act in the two mutually perpendicular directions in which there are no shear stresses. The maximum shear stress is equal to OA and acts in a direction at 45 degrees to the direction of the principal stresses.

In Figure 6 only two dimensions have been considered, whereas there is always a third principal stress. For the case of an axially symmetrical load such as is considered here, this is the tangential normal stress and has an intermediate value.

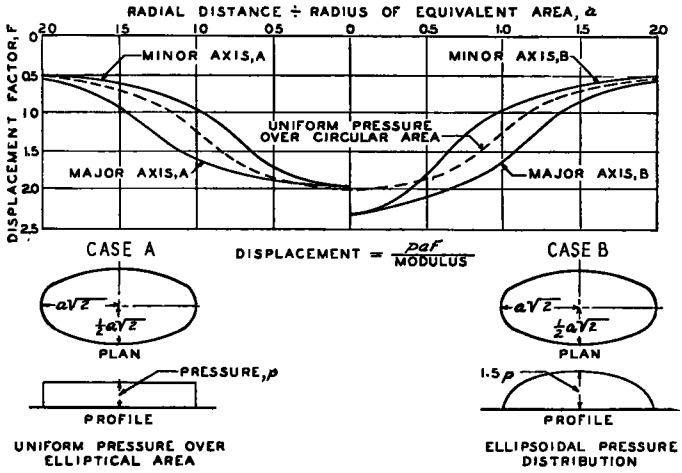

Figure 5. Surface Displacements for Various Pressure Distributions

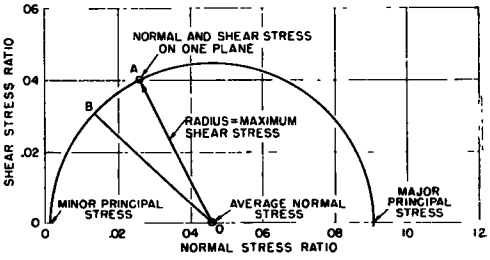

Figure 6. Stresses at a Point

TRIAXIAL SHEAR TEST

The stresses at a point in a loaded soil mass may be simulated in a cylindrical sample by applying normal stresses to its faces by means

of an apparatus such as that shown in Figure 7. The stress on the ends of the cylinder corresponds to the major principal stress. The stress on the curved face corresponds to the minor principal stress. The intermediate principal stress is the same as the minor principal stress, which, although an arbitrary condition, is satisfactory since it is the severest condition possible and has a minor effect. While compressive stresses are applied, the sample fails by shearing so that the test has been called both triaxial compression and triaxial shear.

To evaluate a subgrade material by means of this test, a sample may be taken from the

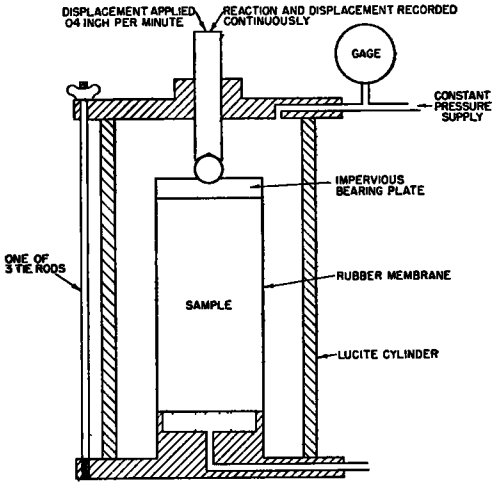

Figure 7. Essentials of Triaxial Shear Test

subgrade in an undisturbed condition or prepared so as to simulate the worst conditions expected to obtain during the life of the structure and for which it is economical to design. Evaluation of field conditions is a problem in itself, involving observations at various locations of moisture, density, and temperature variations with time and analysis of their relationship to soil and pavement properties, climate, topography, ground water and loading.

The sample is placed in a rubber membrane, which is clamped to two rigid end plates, the lower of which is connected to a drain. (If desired, the drain may be closed to prevent drainage from the sample). The lucite cylinder and loading head are assembled and tightened, and the head of the testing machine is brought just in contact with the piston. A constant pressure is applied to the chamber around the sample and is designated lateral pressure, L. The reaction indicator of the testing machine is set to zero. The piston is displaced at a rate of 0.04 in. per minute and the reaction and displacement recorded. The test is continued until the reaction becomes constant or diminishes. The vertical pressure, V, minus the lateral pressure, L, is calculated from the reaction, R, the reduction in height per unit height, d, and the initial cross-sectional area of the test sample by the relation $V - L = \frac{R - dR}{A}$.

TABLE 3
REPORT OF TRIAXIAL COMPRESSION TEST RESULTS

Vertical minus lateral pressure, V-L	Lateral pressure, L,—*kips per sq ft*		
	0	2	4
	Reduction in height, *d*		
kips per square foot	*percent*	*percent*	*percent*
0	0.0	0.0	0.0
Lateral pressure applied			
0	0 0	0.2	0.3
1	0.3	0.4	0.45
2	1.0	1.0	0.9
3	2.5	2.3	1.8
4	6.0	5.0	4.5
Maximum V-L, kips per sq ft	4.3	4.5	5.0
Corresponding *d*, percent	10	16	17
Initial density, lb per cu ft...	124	126	126
Initial moisture content, percent of dry soil	21.8	22.3	22.5
Initial density (dry weight) lb per cu ft..	102	103	103

Separate samples are tested with different lateral pressures to evaluate the effect of this variable. Its effect on the maximum reaction may also be determined from one sample for materials which are not brittle by retesting the sample at a higher lateral pressure.

The results of tests on three samples taken from a compacted clay subgrade are shown in Table 3. For the three values of L, $V - L$ is plotted against d in Figure 8*A*. The reduction in height due to L, for $V - L = 0$, represents volume change (0.2 percent for $L = 2$ and 0.3 percent for $L = 4$) and is not plotted in Figure 8*A*, which is intended to represent the effect of distortion or lateral displacement. The curves for lateral pressures of 0, 2, and 4 kips per sq ft are not far apart and

an average curve will be used to calculate a modulus of elasticity.

For sand, $V - L$ is approximately proportional to L, making the construction of one effective curve a function of L and therefore a function of the field loading to be considered.

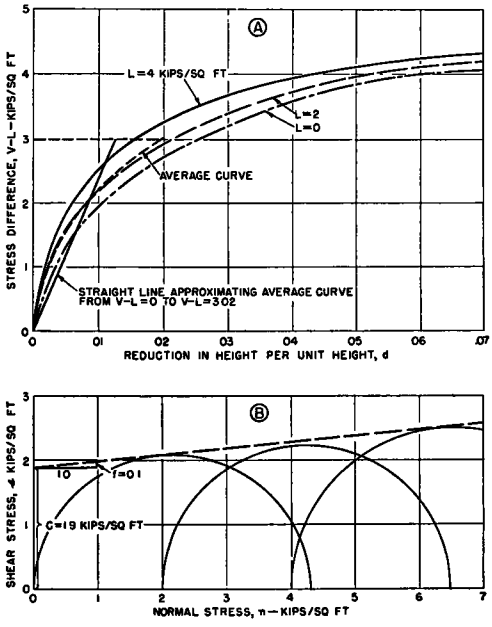

Figure 8. Plot of Triaxial Compress on Test Results

Stress semicircles based on the principle of Figure 6, using L and the maximum V-L from Table 3, are plotted in Figure 8B. The minor principal stress is L and V-L equals the difference in principal stress which is the diameter of the stress circle. The circles have their centers on the horizontal axis at $L + \frac{V-L}{2}$ and pass through L plotted on the same axis. A straight line approximating the envelope of these semicircles defines a relation between the normal stresses and shear stresses on the planes of failure of the test cylinders. (The line is not tangent to all three semicircles due to variations in the samples). The intercept of this line on the vertical axis is termed the cohesion, c, and its slope is the coefficient of internal friction, f. (The angle of internal friction is arc tan f).

THICKNESS OF PAVEMENT AND SETTLEMENT

The vertical displacement factors for points below the center of a uniform pressure applied over a circular area are plotted in Figure 9 for Poisson's ratio = 0.5. The maximum stress difference at any depth is also shown. These curves may be used to calculate the maximum displacement due to distortion below any depth for a given load on a cohesive subgrade for which triaxial compression test results are available.

Settlement due to volume reduction could be calculated separately. However, since

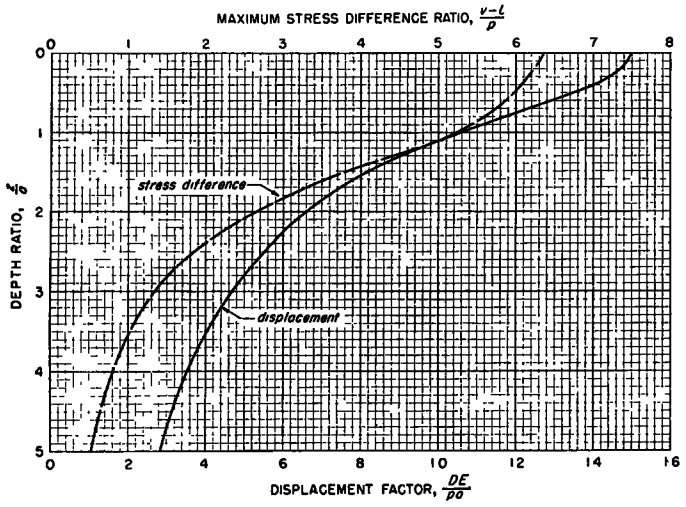

Figure 9. Vertical Displacement and Stress Difference at Different Depths

volume reduction strengthens the soil, the resulting settlement is usually not critical in pavement thickness design for distributed traffic and is not calculated here.

For example, assume a load $P = 10$ kips with a unit pressure $p = 8.64$ kips per sq ft (60 lbs per sq in) and calculate the displacement at a depth of 1 ft for a subgrade represented by the test results shown in Table 3 and Figure 8.

Now, the equivalent radius, a, of the area over which the load is applied is calculated as follows: $a = \sqrt{\frac{P}{\pi p}} = \sqrt{\frac{10}{3.14 \times 8.64}} = 0.607$ ft.

At a depth of 1 ft, $\frac{z}{a} = \frac{1}{0.607} = 1.65$.

From Figure 9, for $\frac{z}{a} = 1.65$, $\frac{V-L}{p} = 0.35$ and $\frac{SE}{pa} = F$ (as defined in Table 2) $= 0.78$.

Then, $V\text{-}L = 0.35p = 0.35 \times 8.64 = 3.02$ kips per sq ft.

In Figure 8A, a straight line is drawn to approximate the average of the test curves from $V\text{-}L = 0$ to $V\text{-}L = 3.02$ by making the area between the vertical axis and the straight line equal to the area between this axis and the average curve. The slope of the straight line is taken as the effective modulus of elasticity, E, for the subgrade. Using the ordinate on this line at $d = 0.01$ gives $E = \frac{2.35}{.01} = 235$ kips per sq ft.

Since $\frac{SE}{pa} = 0.78$, the displacement at a depth of 1 ft is $S = \frac{0.78pa}{E} = \frac{0.78 \times 8.64 \times 0.607}{235} = 0.0174$ ft or 0.21 in.

If an allowable displacement is determined from field observations, similar calculations would determine the depth, z, in the subgrade at which this displacement would occur. Since E depends on the depth, z, it is generally most convenient to calculate S for various assumed values of z and plot z against S to determine z for given values of S. Thus for the above conditions, at $z = 1.5$ ft, $S = 0.110$ in, and at $z = 2$ ft, $S = 0.064$ in. For an assumed allowable displacement of $S = 0.1$ in, $z = 1.6$ ft by interpolation.

For a flexible pavement with a modulus E_p equal to that of the subgrade, this depth would be taken as the required pavement thickness (surface plus base). If E_p is greater than E, the pavement thickness, t, could be calculated from the formula (*13*):

$$t = z \sqrt[3]{\frac{E}{E_p}}$$

For several layers with different moduli, each layer can be considered as an equivalent thickness of subgrade.

For example, the Kansas Highway Department has used the foregoing analysis (*14*) for calculating pavement thickness using $E_p = 2{,}160$ kips per sq ft and $S = 0.1$ in. Using this value of E_p and $E = 330$ corresponding to $z = 1.6$ ft, the required pavement thickness is

$$t = 1.6 \sqrt[3]{\frac{330}{2160}} = 0.855 \text{ ft} = 10.3 \text{ in}$$

For granular materials the modulus varies appreciably with the lateral pressure making it difficult to select an effective value of the modulus. For example, a base course material conforming to the AASHO specifications gave a modulus of 500 kips per sq ft with a lateral pressure of 1 kip per sq ft and 1000 kips per sq ft with a lateral pressure of 2 kips per sq ft. Field correlations may make it possible to determine an effective lateral pressure to use in evaluating such materials.

THICKNESS AND OVERSTRESS OF A POINT

By plotting the stress ratios from Table 1 in the manner shown in Figure 6, the various combinations of cohesion and friction required to prevent overstress at points at various depths were calculated (*15*) and are plotted in Figure 10. Thus, for $p = 8.64$ kips per sq ft and $\frac{z}{a} = 1.65$ as in the previous example, and with $f = 0.1$ from Figure 8B, $\frac{c}{p}$ from Figure 10 is 0.16. Then the cohesion required to prevent overstress of any point in the subgrade below a depth of 1 ft is $c = 0.16 \times 8.64 = 1.38$, which is to be compared with the test value of 1.9 from Figure 8B, giving a factor of safety of $\frac{1.9}{1.38} = 1.38$. For a factor of safety of 1, $\frac{c}{p} = \frac{1.9}{8.64} = 0.22$, which, from

Figure 10, gives $\frac{z}{a} = 1.0$ or $z = 1 \times 0.607$ ft or 7.3 in. Neglecting pavement rigidity this is the minimum allowable thickness. Comparison of this design method with field observation has been reported from Great Britain (*16*), indicating its applicability to cohesive subgrades.

Overstress at a point occurs at a considerably lower pressure than the bearing capacity which corresponds to total failure for a single loading; however, a large number of repetitions of a load which causes overstress at a point in a clay or loose sand may eventually cause failure by progressive deterioration. In dense sands this criterion is invalid because such a material tends to expand before failure so that the stresses are redistributed from a region which is approaching overstress until the bearing capacity is reached, whereupon the sand fails sharply in a manner typical of brittle materials.

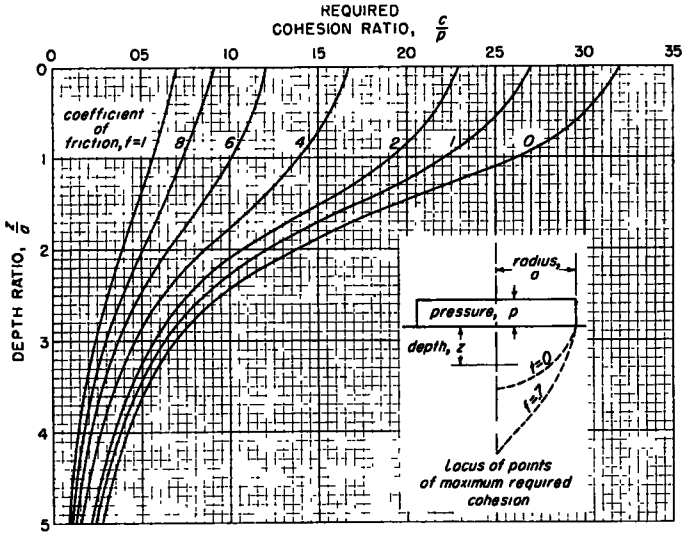

Figure 10. Depth Required to Prevent Overstress of a Point

THICKNESS AND BEARING CAPACITY

The vertical pressure transmitted through the pavement may be compared with the bearing capacity of the subgrade (*17*) as indicated in Figure 11. The ratio of the maximum vertical pressure, p', at any depth to the applied, pressure, p is plotted in Figure 12 from Table 1. The pressure distribution on horizontal planes is not uniform but may be approximated for the present purpose (see Fig. 11) by a uniform pressure equal to p' distributed over an area of radius a' such that the total load at any depth is equal to the load applied at the surface. The ratio $\frac{a'}{a}$ is given in Figure 12.

For illustration, again take $z = 1$ ft, a = 0.607 ft, $\frac{z}{a} = 1.65$, $p = 8.64$ kips per sq ft, $f = 0.1$, and $c = 1.9$ kips per sq ft; find the

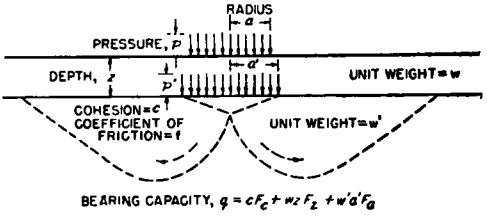

f	F_c	F_a	$F_{a'}$
0	74	00	00
1	9	08	01
2	14	21	04
3	19	43	12
4	27	8	30
5	36	14	66
6	53	24	13
7	75	40	26
8	106	67	51
9	156	108	102
10	224	172	192

Figure 11. Bearing Capacity Under Circular Loaded Area

unit weight of the subgrade $w' = 125$ lb per cu ft or 0.125 kips per cu ft, which is the initial density given in Table 3; and assume the density of the pavement $w = 0.140$ kips per cu ft. From Figure 12, for $\frac{z}{a} = 1.65$, $\frac{a'}{a} = 1.63$ and $a' = 1.63 \times 0.607 = 1.0$ ft; also, $\frac{p'}{p} = 0.375$ and $p' = 0.375 \times 8.64 = 3.24$ kips per sq ft. Now the bearing capacity, q, may be computed from the formula and factors given in Figure 11. Thus, for $f = 0.1$, $F_c = 9$, $F_z = 0.8$, $F_a = 0.1$, and $q = 1.9 \times 9 + 0.140 \times 1 \times 0.8 + 0.125 \times 1.0 \times 0.1 = 17.1 + 0.11 + 0.01 = 17.2$ kips per sq ft. Now, q may be compared with p' giving a factor of safety against total failure of the subgrade of $\frac{17.2}{3.24} = 5.3$.

For a given factor of safety, the required depth may be calculated by trial. Thus for a factor of safety of 3, the required thickness of nonrigid pavement or required effective depth of cover is $z = 7$ in.

For a cohesive material with a low value of f as above, the bearing capacity is approximately cF_c and the depth and size of loaded area have only a small effect. For sand the reverse is true. Thus, for a moderately compact sand we might have $c = 0$, $f = 0.8$, and $w' = 0.105$ kips per cu ft, so that with the above dimensions $q = 0 + 0.140 \times 1 \times 67 + 67 + 0.105 \times 1.0 \times 51 = 0 + 9.4 + 5.4 = 14.8$ kips per sq ft. Values of q would be higher for greater values of f which would result from increased compaction.

This method of design has been used extensively (*18*) except that the bearing capacity of the subgrade is here calculated from triaxial compression test results instead of being assumed or derived from field loading tests.

EFFECT OF MOISTURE

The effect of moisture content of a single clay subgrade material on pavement thicknesses calculated by the three foregoing methods is shown in Table 4. The calculated thickness depends, of course, upon the allowable settlement or required factor of safety against overstress, which in turn can only be determined by correlation of analyses of test results with pavement performance. In Table 4, $P = 10$ kips, $p = 8.64$ kips per sq

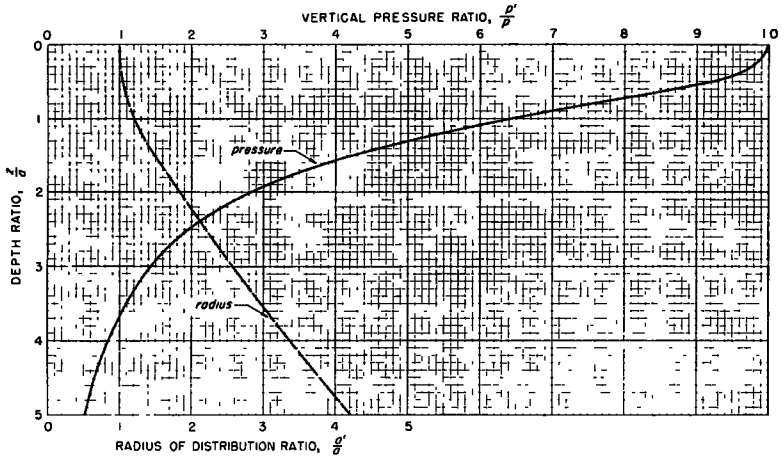

Figure 12. Vertical Pressure Distribution

TABLE 4
EFFECT OF MOISTURE CONTENT OF CLAY SUBGRADE ON CALCULATED PAVEMENT THICKNESS

Moisture content	Design criterion		
	Displacement	Point overstress	Bearing capacity
	Pavement thickness for 10-kip wheel load		
	in.	*in.*	*in.*
14	0	0	0
19	4 2	0	4.5
23	9.8	8.6	8.0
26	12.5	15.1	13.6

ft; for the displacement method, $S = 0.2$ in. and $E_p = 2{,}160$ kips per sq ft; for point overstress, a factor of safety of one is used; for bearing capacity, a factor of safety of 3 is assumed.

These analyses consider vertically applied pressures only. Therefore, the zero pavement thicknesses calculated for a moisture content of 14 percent does not indicate that no cover is required to take care of abrasive stresses. Furthermore, if such a soil were left unloaded in a humid climate, it would become much wetter and weaker. In fact, the pavement may have more effect on the strength of the subgrade than it does on the stresses transmitted to the subgrade. The moisture content of 26 percent was obtained by compacting samples to the AASHO maximum density and optimum moisture content and then allowing them to sorb water while confined by an all-around pressure equivalent to a head of one foot of water.

EFFECT OF LOAD

For a constant unit pressure, the variation of pavement thickness with load calculated by the displacement method depends upon the variation of the allowable settlement with the wheel load. For instance, if the allowable S is assumed proportional to a, then t is proportional to $\sqrt{P}$. For S independent of the load, t increases much more rapidly with increased load.

For a constant factor of safety in the point overstress method, t is proportional to $\sqrt{P}$ if a constant strength of soil is assumed. However, as the pavement thickness increases, it may be expected that the minimum seasonal strength of the subgrade will increase so that t would actually increase less rapidly than $\sqrt{P}$.

Using a factor of safety of 3 against bearing capacity for the clay at 26 percent moisture with $c = 1.1$ and $f = 0$, and for sand with $c = 0$ and $f = 0.8$, pavement thicknesses for various wheel loads and $p = 8.64$ kips per sq ft are given in Table 5. It may be seen that for the clay t is proportional to $\sqrt{P}$ but for the sand, the rate of increase is much smaller.

BRAKING STRESSES

In addition to vertical pressures, the stopping of vehicles causes shear stresses, s, on the surface in the direction of travel. The magnitude of s depends upon the rate of deceleration and is limited by the product of the vertical pressure and the coefficient of friction between the tire and the surface.

TABLE 5
EFFECT OF TYPE OF SUBGRADE ON VARIATION OF PAVEMENT THICKNESS WITH WHEEL LOAD BASED ON BEARING CAPACITY

Wheel load	Clay subgrade	Sand subgrade
	Pavement thickness	
kips	*in*	*in.*
5	9.5	8.3
10	13.6	10.0
15	16.6	10.9
20	19 2	11.5
30	23.6	12.3
60	33.3	13.3

The stresses transmitted from such a surface shear stress may be of use to indicate the required thickness and strength of the surface course. For instance, the horizontal shear stress, s_h, near the contact of a surface course with a base course may be a factor in the required thickness of surfacing or the required strength of the materials near the

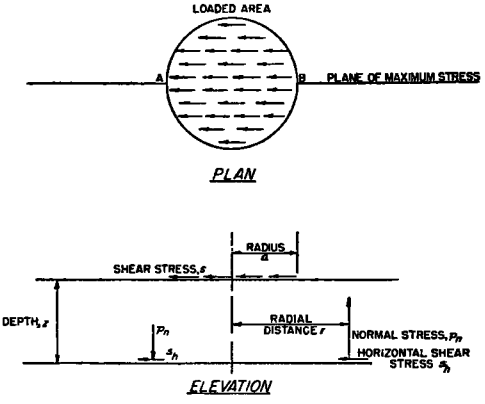

Figure 13. Stresses From Applied Shear Stress

plane of contact. For a uniform shear stress, s, applied over a circular area at the surface as shown in Figure 13, the maximum values of s_h are in the vertical plane through the center of the circle and oriented in the direction of travel.

It so happens that the ratio $\frac{s_h}{s}$ is the same numerically as $\frac{p_r}{p}$ for Poisson's ratio = 0.5

for a vertically applied load (9) as tabulated in Table 1. Thus, for $\frac{z}{a} = 0.5$, the maximum value of $\frac{s_h}{s}$ is 0.374 at $\frac{r}{a} = 0$, so that the maximum shear stress in a horizontal direction at the depth $z = 0.50$ has been reduced to 37 percent of its values at the surface.

The normal stress on a horizontal plane, p_n, is compressive in front of the area to which shear stresses are applied but tensile behind the center of the loaded area. The ratio $\frac{p_n}{s}$ is equivalent numerically to $\frac{s_r}{p}$ given in Table 1. The maximum tensile stress is at the edge of the loaded area (point B in Figure 13) where $\frac{p_n}{s} = 0.318$. At a depth $\frac{z}{a} = 0.5$, the maximum value of $\frac{p_n}{s} = 0.262$, as shown in Table 1 at $\frac{r}{a} = 1.0$. The horizontal normal stress developed by an applied shear stress is likewise compressive in front of the loaded area and tensile behind it. Its magnitude is theoretically infinite at points A and B.

The stresses transmitted from a combination of vertical and shear loads may be calculated as the sum of corresponding stresses calculated for each load separately.

The maximum resistance of a surface to horizontal displacement is the sum of its horizontal bearing capacity, Q_h, and the total shearing resistance, S_b, at its lower boundary. For the shear loading considered above, Q_h, is approximately $4\ acz + 1.4cz^2$, where c is half the compressive strength of a cohesive surface; and $S_b = s_b \pi a^2$ where s_b is the unit shearing resistance at the lower boundary. Equating $Q_h + S_b$ to the applied shear force, $s\pi a^2$, and solving for z gives approximately $z = \frac{2}{3}\ a\ \frac{s - s_b}{c}$ as the thickness of surface required to prevent failure by horizontal displacement.

The value of s cannot exceed c because skidding is imminent for $s = c$. For the worst condition $s_b = 0$ and $s = c$ so that $z = \frac{2}{3}a$ which gives for a 10-kip load with $a = 0.607$ ft, $z = \frac{2}{3} \times 0.607 = 0.4$ ft or 5 in. With c greater than s or with an appreciable value of s_b, the required thickness would be reduced. Thus, for the above loading and $c = 2s$, $z = 2.5$ in. for $s_b = 0$ or $z = 0.5$ in. for $s_b = 0.8s$. If the surface is laminated, the same analysis could be applied to the upper layer of the surface.

SUMMARY

Tables and graphs of stresses, displacements, and bearing capacity under normal and tangential surface loads have been presented. Their application to the design of thickness of flexible pavement courses is outlined using unit values for the components derived from triaxial compression tests. Designs based on allowable displacement, overstress at a point and total failure have been considered. These analyses are not proposed as determinative design procedures but are rather intended as an aid in studying the behavior of pavements in service, and as a guide in planning and conducting experimental studies of the interaction of pavements and subgrades.

REFERENCES

1. Love, A. E. H., "The Stresses Produced in a Semi-Infinite Solid by Pressure on Part of the Boundary," Philosphical Transaction of the Royal Society, Series A, Vol. 228 (1929).
2. Tufts, Warner, "Public Aids to Transportation," Vol. IV, Report of the Federal Coordinator of Transportation, Appendix p. 248 (1940).
3. Newmark, N. M., "Influence Charts for Computation of Stresses in Elastic Foundations," University of Illinois Engineering Experiment Station Bulletin 338 (1942).
4. Biot, M. A. and Clingan, F. M., "Consolidation Settlement of a Soil with an Impervious Top Surface," *Journal of Applied Physics*, July, 1941.
5. Haskell, N. A., "The Motion of a Viscous Fluid Under a Surface Load," *Physics*, p. 265, Aug. 1935, and p. 56, Feb., 1936.
6. Terzaghi, Karl, "Theoretical Soil Mechanics," John Wiley & Sons, p. 389, (1943).
7. Timoshenko, S., "Theory of Elasticity," McGraw-Hill Book Co., pp. 339 and 349, (1934).
8. Markwick, A. H. D. and Starks, H. J. H., "Stresses Between Tire and Road," *Journal of the Institution of Civil Engineers*, June, 1941.
9. Westergaard, H. M., "Effect of a Change of Poisson's Ratio Analyzed by Twinned

Gradients," *Journal of Applied Mechanics*, Sept., 1940.
10. Spangler, M. G., "Wheel Load Stress Distribution Through Flexible Type Pavements," *Proceedings*, Highway Research Board, Vol. 21, p. 110 (1941).
11. Way, Stewart, "Some Observations on the Theory of Contact Pressure," *Journal of Applied Mechanics*, Dec., 1940.
12. Teller, L. W. and Buchanan, J. A., "Determination of Variation in Unit Pressure over the Contact Area of Tires," *Public Roads*, Dec., 1937.
13. Burmister, D. M., "The Theory of Stresses and Displacements in Layered Systems and Applications to the Design of Airport Runways," *Proceedings* Highway Research Board, Vol. 23, p. 126, and Discussion, p. 146 (1943).
14. Worley, H. E., "Triaxial Testing Methods Usable in Flexible Pavement Design," *Proceedings* Highway Research Board, Vol. 23, p. 109 (1943).
15. Barber, E. S. and Mershon, C. E., "Graphical Analyses of the Stability of Soil," *Public Roads*, October, 1940.
16. Glossop, G. and Golder, H. Q., "The Construction of Pavements on a Clay Foundation Soil," Paper of Road Engineering Division of the Institution of Civil Engineers, 1944.
17. Terzaghi, Karl, "Theoretical Soil Mechanics," John Wiley & Sons, p. 125 (1943).
18. Kersten, M. S., "Review of Methods of Design of Flexible Pavements," *Proceedings* Highway Research Board, Vol. 25, p. 8 (1945).

DESIGN OF FLEXIBLE SURFACES IN MICHIGAN

W. W. McLAUGHLIN AND O. L. STOKSTAD
Michigan State Highway Department

SYNOPSIS

A discussion of Michigan's basis for design describing how design criteria have been developed around a system of soil profile classification is presented. Traffic volumes control wearing course design, and soil, drainage, and climate are important factors controlling foundation design. The relations between laboratory test results and the soil classification based on field study of soil profiles is also discussed.

The soil survey provides most of the soil engineering design information. In addition to this it supplies area meaning by which to test results; it yields information concerning the natural environment of the samples collected; and it suggests the influence which changes in this environment will have on the significance of test results. Information obtained both from laboratory tests and from field identification of soils is complementary in providing a soil engineering background for the design of flexible surfaced roads.

In considering design of flexible highway surfaces it is natural and desirable that a great deal of attention should be devoted to the development of tests for determining the thickness of sub-base, base and surfacing. A number of sampling and testing methods have been developed for this purpose, some of which are the California bearing ratio test, North Dakota cone test, Florida sand test, and various shear tests. Each of these are intended to yield information for specific design problems after the location has been selected and grades established. As yet, however, there is no complete agreement or general acceptance of any method of rational foundation design for flexible surfaces.

In Michigan, field studies rather than laboratory studies have been emphasized as a basis for design. These studies combined with long experience in the evaluation of soil, geology, climate, water, and certain laboratory tests as factors in foundation design, serve to determine the practices to be followed. This method has been successful for two reasons. First, highway wheel loads have remained fairly constant, so that experience of 15 years ago is still applicable insofar as the effect of this factor on foundation